Published online 28 November 2006 *Nucleic Acids Research, 2006, Vol. 34, No. 22* ***6561–6573***
doi:10.1093/nar/gkl941

Cellular delivery of small interfering RNA by a non-covalently attached cell-penetrating peptide: quantitative analysis of uptake and biological effect

Sandra Veldhoen, Sandra D. Laufer, Alexander Trampe and Tobias Restle*

Institut für Molekulare Medizin, Universitätsklinikum Schleswig-Holstein, Universität zu Lübeck, Ratzeburger Allee 160, 23538 Lübeck, Germany

Received October 9, 2006; Accepted October 18, 2006

ABSTRACT

Cell-penetrating peptides (CPPs) have evolved as promising new tools to deliver nucleic acids into cells. So far, the majority of these delivery systems require a covalent linkage between carrier and cargo. To exploit the higher flexibility of a non-covalent strategy, we focused on the characterisation of a novel carrier peptide termed MPGα, which spontaneously forms complexes with nucleic acids. Using a luciferase-targeted small interfering RNA (siRNA) as cargo, we optimised the conditions for MPGα-mediated transfection of mammalian cells. In this system, reporter gene activity could be inhibited up to 90% with an IC_{50} value in the sub-nanomolar range. As a key issue, we addressed the cellular uptake mechanism of MPGα/siRNA complexes applying various approaches. First, transfection of HeLa cells with MPGα/siRNA complexes in the presence of several inhibitors of endocytosis showed a significant reduction of the RNA interference (RNAi) effect. Second, confocal laser microscopy revealed a punctual intracellular pattern rather than a diffuse distribution of fluorescently labelled RNA-cargo. These data provide strong evidence of an endocytotic pathway contributing significantly to the uptake of MPGα/siRNA complexes. Finally, we quantified the intracellular number of siRNA molecules after MPGα-mediated transfection. The amount of siRNA required to induce half maximal RNAi was 10 000 molecules per cell. Together, the combination of methods provided allows for a detailed side by side quantitative analysis of cargo internalisation and related biological effects. Thus, the overall efficiency of a given delivery technique as well as the mechanism of uptake can be assessed.

INTRODUCTION

Today there is a fast growing number of nucleic acid-based strategies to modulate a vast variety of cellular functions [for a review see: (1)]. Several classes of oligonucleotides like aptamers, transcription factor-binding decoy oligonucleotides, ribozymes, triplex-forming oligonucleotides, immunostimulatory CpG motifs, antisense oligonucleotides (including peptide nucleic acids), small interfering RNAs (siRNAs) and microRNAs have attained much interest as a research tool owing to their highly specific mode of action. Even more important, these oligomeric nucleic acids do have a considerable potential to be used as therapeutics. However, the bottleneck of any nucleic acid-based strategy remains the cellular delivery of these macromolecules. Essentially, the nucleic acid delivery techniques available today comprise various physical and chemical methods, viral and non-viral vector systems, and uptake of naked nucleic acids. They all have certain advantages and disadvantages and might only be appropriate if particular requirements are fulfilled. In general, physical and chemical methods like microinjection, electroporation or particle bombardment as well as calcium phosphate co-precipitation are highly efficient but rather harmful for the target cells and lack the potential to be applicable *in vivo*. There is general consent that viral vector systems are the most efficient vehicles to deliver nucleic acids into cells. However, despite substantial efforts over the last 15 years, up to now research has failed to develop suitable and especially safe viral systems [for a review see: (2,3)]. On the contrary, the field has experienced several setbacks causing important clinical trials to be put on hold (4–6). As a result of the difficulties encountered with these viral vectors (e.g. mutagenesis and immune responses) much attention was paid to the development of allegedly safer non-viral delivery systems. This conception includes an assortment of fairly unrelated approaches yielding various degrees of enhanced cellular uptake of nucleic acids. Currently, cationic lipids and polymers are used as a standard tool to transfect cells *in vitro*.

*To whom correspondence should be addressed. Tel: +49 451 500 2745; Fax: +49 451 500 2729; Email: restle@imm.uni-luebeck.de

The authors wish it to be known that, in their opinion, the first two authors should be regarded as joint First Authors

However, these approaches are commonly characterised by a significant lack of efficiency accompanied by a high level of toxicity and thus rendering them mostly inadequate for *in vivo* applications. Nonetheless, there are a few studies reporting a successful delivery of siRNA *in vivo* applying cationic liposomes (7,8), atelocollagen- or PEI-complexed siRNAs (9–12) as well as cholesterol-conjugated siRNAs (13,14). Peptides, on the other hand, acting as shuttles for a controlled cellular delivery of nucleic acids, represent a new and innovative concept to bypass the problem of poor bio-availability of these macromolecules. The idea of using peptides as carriers goes back some 18 years, when two groups discovered by chance that the HIV-1 transactivating protein Tat is taken up by mammalian cells (15,16). Just a few years later, the Antennapedia homeodomain of *Drosophila melanogaster* was shown to act similarly (17). Further on, it could be shown that peptides derived from Tat and Antennapedia as well as other proteins are capable of transporting macromolecular cargo molecules into cells (18–20). Based on such promising results, a rapidly expanding field focusing on the so-called cell-penetrating peptides (CPPs) began to develop. Up to now numerous additional peptides have been reported to show cell-penetrating properties and many of them have been used to successfully deliver a variety of macromolecular cargos into cells [for a review see: (21,22)].

For all the sequence diversity, CPPs share some common features beside their ability to cross biological membranes: (i) a high content of basic amino acids, and (ii) a length of 10–30 residues. Two strategies are utilised for the attachment of cargo molecules. By far the majority of studies include a covalent attachment of carrier and cargo [for a review see: (23)]. This approach might be effective for a specific application (e.g. a particular nucleic acid cargo), but it is fairly limited in terms of flexibility, as a new construct has to be generated for any given nucleic acid cargo. Alternatively, the positive charges of certain amphipathic CPPs can be exploited to bind anionic cargo molecules like nucleic acids non-covalently via ionic interactions (24–26). Additional hydrophobic peptide/peptide interactions then drive the maturation of nanoparticles in a sandwich-like assembly reaction. As a result, such a CPP can in principle be combined with any given oligonucleotide.

For many CPPs, the initial interaction with cells is supposed to be mediated by negatively charged glycosaminoglycan (GAG) receptors of the extracellular matrix, e.g. heparan sulphate proteoglycans (27–33). However, the mechanisms underlying the cellular translocation of CPPs are poorly understood and subject to controversial discussions. Nonetheless, there is considerable evidence that for many CPPs endocytosis is a major route of internalisation (34–38). On the other hand, there are examples in the literature proposing a direct penetration of the cell membrane independent of any endocytotic pathway (39–45), while others suggest both entry routes are used in parallel or under certain conditions (33,46–49). Furthermore, as at least four basic routes of endocytosis can be distinguished to date (50,51), it seems reasonable to speculate about multiple pathways involved in cellular entry of CPPs. Then again, currently available data are based on studies using a variety of different cell lines and techniques, which renders a direct comparison of different approaches impossible (37,52–54). It has been shown that even minor changes of the physical state of a CPP (e.g. exchange of certain amino acids) can alter translocation properties significantly (41,53). This particularly holds true for the attachment of large cargo molecules (55,56). Thus, it might not be possible to generalise results obtained with a given CPP, and it might be necessary to characterise each carrier/cargo complex individually. If CPPs are intended to be used for therapeutic purposes in the future, it is essential to focus on the attachment of functional cargos and analyse their biological effects inside the cell. Therefore, a quantitative comparison of the total amount of cargo taken up with functionally active cargo is an essential requirement in order to improve delivery. As a prerequisite, there is need for a sensitive method to quantify intracellular amounts of cargo in combination with sensitive and easy to handle reporter systems.

In the present study we used the 27 amino acid peptide MPGα, a derivative of the original MPG peptide (24), as carrier for siRNA delivery. The primary amphipathic peptide is composed of a hydrophobic domain, derived from the N-terminal fusion sequence of the HIV-1 glycoprotein 41, and a hydrophilic domain equivalent to the nuclear localisation sequence (NLS) of the SV40 large T antigen linked by the three amino acid spacer WSQ (57). MPGα differs from the parent peptide by six amino acids in the hydrophobic part and is predicted to adopt a partially helical conformation. The peptide forms stable non-covalent complexes with nucleic acids in solution, which eventually assemble into nanoparticles of different sizes (S.V. and A.T., unpublished data). Utilising this model system, we provide a combination of methods for detailed quantitative analyses of peptide-mediated siRNA internalisation along with its biological effects. To the best of our knowledge, we present for the first time a detailed analysis on the number of siRNA molecules per cell required to observe half maximal inhibition of the target for peptide- versus cationic lipid-mediated delivery. Beyond this, the techniques described here are generally applicable for a characterisation of delivery systems of oligonucleotides.

MATERIALS AND METHODS

Oligonucleotides, peptides and cationic lipids

The siRNAs used throughout this study are unmodified as well as fluorescently labelled oligoribonucleotides with a 3′-overhang of two deoxythymidine nucleotides and were purchased from IBA (Göttingen, Germany). The sequences are described in detail elsewhere: si2B and si-sc, (58); siR206 [Rational *fLUC*, position 206, (59)]; siGL3 and siINV [invGL2, (60)]; siLam [lamin A/C siRNA, (61)]. The peptides were each modified with an acetyl group (Ac) at the N-terminus and a cysteamide group (Cya) at the C-terminus and were synthesised and purified by Jerini AG (Berlin, Germany). The sequences are Ac-GALFLAFLAAA-LSLMGLWSQPKKKRKV-Cya for MPGα and Ac-GALFL-AFLAAALSLMGLWSQPKSKRKV-Cya for MPGα-mNLS. Lipofectamine™ 2000 (LF2000) and Lipofectamine™ Plus were purchased from Invitrogen (Karlsruhe, Germany).

Cell lines and cell culture

HeLa-TetOff cells and 293T cells were cultured in Dulbecco's Modified Eagle Medium with 4500 mg/l glucose. ECV304 cells, a derivative of human urinary bladder carcinoma cell line T-24 (ACC 310 DSMZ, Braunschweig, Germany), were cultured in Medium 199. ECV-GFP-Nuc cells, kindly provided by Marita Overhoff, stably express green fluorescent protein tagged with a NLS (pAcGFP1-Nuc, BD Biosciences Clontech, Heidelberg, Germany) and were cultured in Medium 199 supplemented with 100 μg/ml G418. All media were supplemented with 10% foetal calf serum (FCS) and were purchased from Invitrogen. Cells were cultured as exponentially growing subconfluent monolayers in a humidified atmosphere containing 5% CO_2. To establish cell lines stably expressing firefly luciferase two strategies were followed: (i) HeLa-TetOff cells were transfected with pTRE2hyg-luc (cells and plasmid from BD Biosciences, Heidelberg, Germany) using Lipofectamine™ Plus according to the manufacturer's instructions. Stable transfectants were obtained by selection with culture medium containing 200 μg/ml hygromycin B (Invitrogen). (ii) Stably transfected ECV304 cells were generated using a self-inactivating HIV-1 vector system described by Jármy *et al*. (62). Briefly, 293T cells were transfected with a luciferase-harbouring defective HIV-1 genome and plasmid-encoded packaging functions. Forty eight hours later, viral particles were harvested from the culture supernatant by filtration through a 0.45 μm filter and used to infect 10^6 ECV304 cells for 1 h at 37°C. The two stable cell lines generated are referred to as HeLa-TetOff Luc (HTOL) and ECV GL3, respectively.

Cell viability and cytotoxicity

Cell viability was determined by a fluorescein diacetate (FDA, Sigma-Aldrich, Deisenhofen, Germany) assay. Non-fluorescent FDA freely diffuses into cells, where it is cleaved by cellular esterases to fluorescein. The amount of fluorescein is thereby proportional to the amount of living cells (63). Cells were washed twice with phosphate-buffered saline (PBS) and then overlaid with 20 μM FDA. Fluorescence measurements were performed in a microplate reader (Fluoroskan Ascent® FL, Thermo Labsystems, Dreieich, Germany).

For specific applications an *in vitro* toxicology assay (TOX-2, Sigma-Aldrich) was performed according to the manufacturer's instructions. This assay relies on the turnover of the sodium salt of [2,3-bis(2-Methoxy-4-nitro-5-sulfophnyl)-2H-tetrazolium-5-carboxyanilide inner salt] (XTT) by mitochondrial dehydrogenases which can be monitored spectrophotometrically.

Delivery of siRNA with LF2000 or MPGα

Twenty four hours prior to transfection, cells were seeded into 12 or 96 well plates (Greiner, Frickenhausen, Germany). Cell numbers were chosen to finally reach 60% confluency for MPGα-mediated delivery and 90% confluency for LF2000-mediated delivery at the time of transfection. LF2000/siRNA complexes were allowed to form in OptiMEM (Invitrogen) according to the manufacturer's protocol with a final concentration of 10 μg/ml LF2000. Peptide/siRNA complexes were formed likewise by mixing the two components at the individually given concentrations or ratios in OptiMEM and added to the cell layer after 1 min incubation at room temperature. In both cases, routinely, the cell culture supernatant was discarded and replaced by medium supplemented with 10% FCS 4 h after the start of transfection. All information concerning incubation times given in the manuscript refer to the time from the beginning of the transfection procedure. For transfections in the presence of inhibitors/effectors of endocytosis (all purchased from Sigma-Aldrich), cells were incubated with the particular compound in OptiMEM at the concentrations given in Table 1.

Table 1. Inhibitors/effectors of endocytosis

Treatment	Concentration	Effect
4°C	—	Inhibition of energy-dependent processes
Chloroquine	100 μM	Inhibits acidification of endosomes
Cytochalasin B	25 μM	Disruption of microfilaments, inhibition of macropinocytosis
Filipin complex	5 μg/ml	Sterol-binding agent, disrupts caveolar structure and function
Monensin	5 μM	Ionophor, inhibits acidification of endosomes and therefore prevents receptor recycling
Nystatin	25 μg/ml	Sterol-binding agent, disrupts caveolar structure and function
Okadaic acid	100 nM	Activation/induction of caveolin-mediated/dependent endocytosis
Sucrose	100 mM	Inhibition of clathrin-mediated endocytosis
Wortmannin	500 nM	PI(3)K-inhibitor, inhibits endosome fusion

The concentrations given in the table are the concentrations used in this study. Additionally, a brief description of the proposed exerted effect on endocytosis is given for each substance.

Determination of luciferase activity

Luciferase activity was quantified 24 h after transfection, subsequent to the determination of cell viability as described above. Luminescence was measured in a microplate reader (Fluoroskan Ascent® FL, Thermo Labsystems, Dreieich, Germany) using 50–100 μl of a buffer containing 28 mM Tricine (pH 7.8), 500 μM ATP, 250 μM coenzyme A, 250 μM D-luciferin, 33 mM DTT, 200 μM EDTA, 15 mM $MgSO_4$, 1.5% (v/v) Triton X-100 and 5% (v/v) glycerol (all reagents purchased from Sigma-Aldrich). The luminescence was normalised to cell viability to account for cell loss due to cytotoxicity or washing procedures.

Quantification of cellular siRNA uptake via liquid hybridisation assay

The detection of siRNA in cellular extracts was performed essentially as described by Overhoff *et al*. (64). Briefly, transfections were carried out as described above in a 12 well format. Four hours after transfection cells were treated three times with heparin (Fluka/Sigma-Aldrich, 15 U/ml in OptiMEM) totalling 1 h at 37°C to remove extracellularly bound peptide/siRNA complexes. Subsequently, cells were detached by trypsination or by incubation in cold PBS. Ten percent of each sample was used to measure luciferase activity while the rest of the sample was subjected to a liquid hybridisation protocol. Cells were pelleted, incubated in PBS containing 1% NP-40 for 10 min on ice followed by total RNA extraction according to standard protocols. The

quantification of the siRNA was achieved by hybridisation with the corresponding ^{32}P-labelled sense-strand for 10 min at 95°C followed by 1 h incubation at 37°C before the samples were resolved by 20% polyacrylamide gel electrophoresis (PAGE) under non-denaturing conditions. After blotting of the gel onto a nylon membrane (Hybond N+, Amersham, Freiburg, Germany), the signals were quantified with a PhosphorImager (Typhoon™ 8600 Variable Mode Imager, GE Healthcare, München, Germany). Absolute amounts of siRNA in the samples were calculated in relation to the included standards. For this purpose, defined amounts of siRNA were added to control cell lysates before the extraction step and treated simultaneously with the other samples. The amounts of total cellular RNA were determined spectrophotometrically and used for normalisation.

Fluorescence microscopy

ECV304, ECV-GFP-Nuc or HeLa cells were seeded in LabTek® Chamber Slides (8 chambers, Nunc, Wiesbaden, Germany) at ~18 000 cells per chamber and incubated for 24 h. Then cells were washed twice with OptiMEM and further incubated for 4 h with MPGα mixed with fluorescently labelled RNA in OptiMEM (final volume 400 µl). To remove extracellularly bound complexes, cells were treated with heparin as described above. Staining of the cell nuclei was achieved with Hoechst 33342 (12 µg/ml). Finally, microscopy was performed at room temperature in OptiMEM supplemented with 50 mM HEPES, pH 7.0 (Invitrogen). Confocal images were acquired using a Zeiss LSM510 Meta device. Semi-confocal images were acquired using a Zeiss Axiovert 200M microscope with ApoTome. For processing and analysis of the images, the LSM510 (Version 3.2SP2) and the AxioVision (Rel. 4.5) software (both Carl Zeiss) were used for confocal and semi-confocal images, respectively. Fluorescence was visualised using filters for excitation/emission at 470/525 nm for Alexa^{488} and GFP-NLS (green fluorescence), 550/605 nm for Cy3 (red fluorescence) and 365/445 nm for Hoechst 33342 (blue fluorescence).

Microinjection

Twenty four hours prior to the experiment, 1×10^6 HeLa-TetOff cells were plated onto glass cover slips (diameter 12 mm) in a 100 mm cell culture dish. The microinjection setup consisted of a FemtoJet express and a Micromanipulator 5171 (Eppendorf, Hamburg, Germany) mounted on an Axiovert 100 (Carl Zeiss). The micropipette (Femtotip, Eppendorf) was loaded with a Microloader (Eppendorf) containing 2–4 µl of either the luciferase harbouring plasmid pTrehygLuc, siR206 or a mixture of plasmid and siRNA in varying concentrations. Working pressure for injections into adherent cells was 90–150 hPa for 0.2–0.3 s. Twenty four hours after microinjection luciferase activity was evaluated as described above.

RESULTS

MPGα mediates delivery of siRNA into mammalian cells

The primary amphipathic peptide MPGα can bind virtually any negatively charged molecule via ionic interactions in a non-specific manner (S.V. and A.T., unpublished data). Thus, in principle this peptide is compatible with almost any given functional oligonucleotide. As RNAi-mediated inhibition of the reporter gene firefly luciferase is currently one of the most widely used approaches to study siRNA delivery, we decided to utilise this approach for our studies with MPGα. In a first step we established two cell lines stably expressing the firefly luciferase, namely HTOL and ECV304 GL3 (ECV GL3). These cell lines were used throughout the study to characterise MPGα-mediated delivery of siRNA. For comparison, we used the commercially available cationic lipid LF2000.

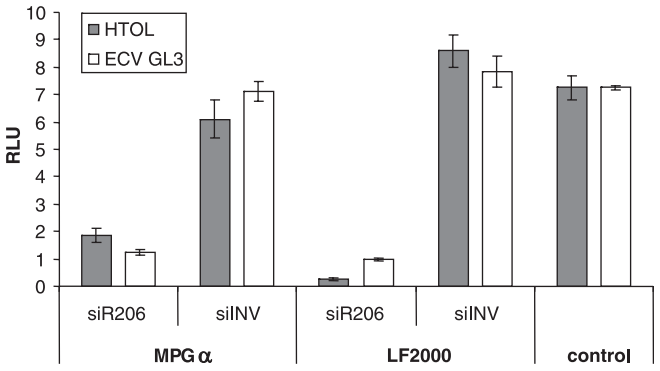

Figure 1. Inhibition of luciferase expression after MPGα- or LF2000-mediated siRNA delivery. Two different cell lines stably expressing firefly luciferase, HTOL and ECV GL3, were transfected in duplicates in a 96 well format with 50 nM siR206 or siINV using 10 µg/ml LF2000 or 4.2 µM MPGα, respectively. Control cells were incubated with OptiMEM only. Luciferase expression given as RLU was measured 24 h after transfection and normalised to cell viability. The graph shows one representative experiment. Luciferase activity is reduced by 70 and 97% in HTOL cells and 83 and 88% in ECV GL3 cells after MPGα- or LF2000-mediated delivery of siR206, respectively.

Figure 1 shows that MPGα translocates sufficient molecules of the siRNA siR206 (59) into reporter gene expressing cells to induce a pronounced reduction of the luciferase activity. Similar results were obtained when using the anti-luciferase siRNA siGL3 (60) (data not shown). Irrespective of the cell line used, we observed a maximal extent of siRNA-mediated inhibition of 80–90% of the target gene expression, which was equal to or even higher than levels reached with LF2000. The transfection procedure was rather straightforward. Briefly, complexes of carrier and cargo were formed by simple mixing of MPGα and siRNA in OptiMEM. After a short incubation for 1–3 min, the mixture was added to the cells for a transfection period of 4 h. Then, the mixture was removed followed by the addition of fresh medium supplemented with FCS and the luciferase activity was measured 20 h later. Hereby, it was irrelevant if peptide and nucleic acid were mixed at the desired final concentrations or the final concentration was adjusted by sequential dilution of a concentrated carrier/cargo solution (data not shown). To ensure that the incubation of cells with the peptide/siRNA complexes *per se* did not influence luciferase expression, additional siRNAs were used as controls. Neither si2B, targeted to ICAM-1, nor the corresponding scramble control si-sc (58) or siINV (60), both without a cellular target, did show any significant change in luciferase activity when compared to non-transfected control cells (Figure 1

and Supplementary Figure 1A). The same was true for LF2000-mediated transfections, evidently excluding any unspecific effects. As LF2000 and to a certain extent also MPGα proved to be toxic at higher concentrations, it was necessary to take this into account. Thus, in each experiment the values of luciferase activity measured were normalised for different cell viabilities with the help of a FDA assay, which was carried out immediately prior to each luminescence measurement.

An overall positive net charge is supposed to be a prerequisite for the initial interaction of the carrier/cargo complexes with negatively charged cell surface components. Accordingly, the optimal ratio of peptide to nucleic acid was determined. When siRNA was mixed at a concentration of 50 nM with increasing concentrations of MPGα (1.3–12.6 μM), best results were achieved at an excess ratio of positive charges of 15 (Supplementary Figure 1B). The optimal concentration of the peptide was determined to be 2–4 μM. In this range, no significant cellular toxicity occurred as determined via the XTT assay (data not shown). During optimisation of the transfection protocol, we observed that cell density at the time of transfection plays an important role for transfection efficiency. For transfections with MPGα the maximum RNAi effect was observed at cell densities of 60–70%, whereas with LF2000 >90% confluency of the cells at the time of transfection gave the best results (data not shown).

Recently it was shown by Simeoni *et al*. (39) that a fluorescently labelled siRNA localised rapidly into the nucleus when transfected with MPG, a related peptide described by Morris *et al*. (24). Interestingly, the authors further reported about a cytoplasmatic localisation when the C-terminal SV40 large T-antigen NLS sequence was mutated. Since both peptides MPG and MPGα share the same C-terminal NLS sequence, we were wondering if comparable results are to be seen with MPGα. However, we could not observe any differences between MPGα and a corresponding peptide harbouring a lysine to serine mutation at position two of the NLS sequence (MPGα-mNLS) neither by microscopic studies nor analysing the luciferase activity (data not shown).

In order to compare the transfection efficiency of MPGα with that of other delivery agents like LF2000, we determined the apparent value of half maximal inhibition (IC_{50}). In Figure 2 representative dose-response curves are depicted for MPGα- and LF2000-mediated siRNA delivery, respectively. From transfections of both HTOL and ECV GL3 cells with MPGα/siRNA complexes IC_{50} values of ~0.8 nM were calculated (Figure 2A), whereas LF2000-mediated transfections yielded IC_{50} values of 0.02–0.04 nM (Figure 2B). These results gave a first hint that MPGα-mediated delivery of siRNA might be less efficient when compared to LF2000. Consequently, we set out experiments trying to unravel the underlying mechanisms for this observation.

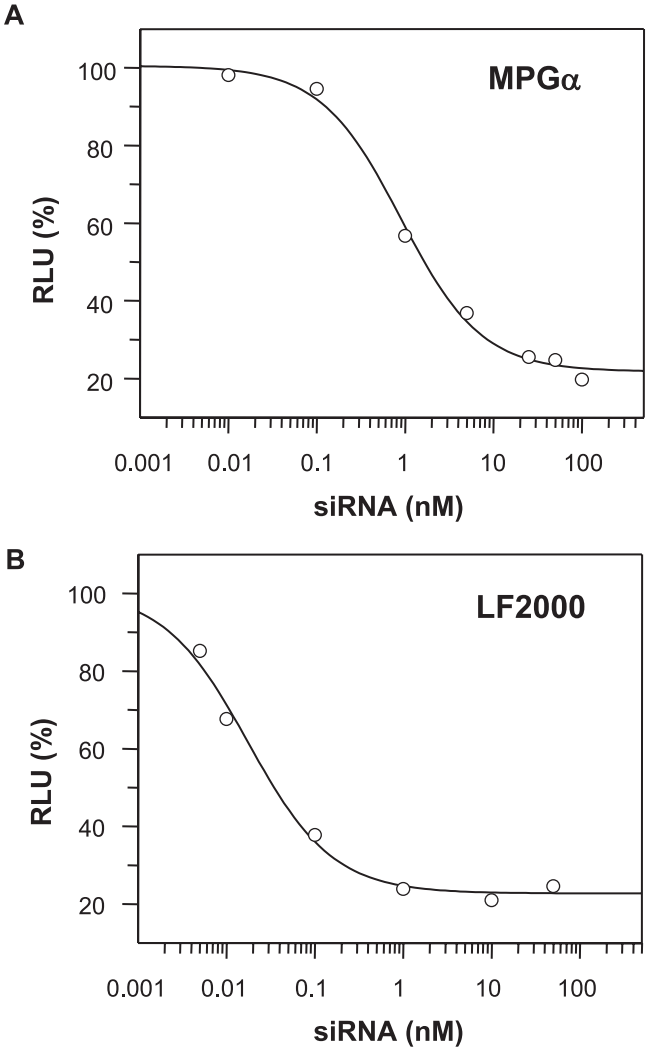

Figure 2. IC_{50} of anti-luciferase siRNA delivered by MPGα and LF2000. ECV GL3 cells were transfected in a 96 well format using a constant concentration of 4.2 μM MPGα (**A**) or 10 μg/ml LF2000 (**B**) and siRNA concentrations varying from 0.005 nM to 100 nM. Luciferase expression given as RLU was measured 24 h after transfection and normalised to cell viability. RNAi-mediated down-regulation of the luciferase activity was expressed as the percentage of active siR206 versus inactive siINV and the IC_{50} value was calculated using the GraFit5 software (Erithacus Software, Surrey, UK). The curves show the best fit of the data of a representative experiment in duplicates which yielded IC_{50} values of 0.89 nM (±0.15) for MPGα (A) and 0.018 nM (±0.004) for LF2000 (B).

Quantification of siRNA internalised

The above described functional siRNA-based delivery assay provided us with the knowledge that MPGα-mediated cellular transfection of a given extracellular quantity of siRNA was less efficient in terms of reporter gene inhibition than LF2000-mediated transfection. One possible explanation for this observation could simply be a lower rate of siRNA internalisation. Alternatively, the amount of bio-available siRNA molecules inside the cell could be lower due to insufficient release from the carrier/cargo complexes and/or trapping of complexes in particular cellular compartments. To investigate this issue in more detail, we analysed the amount of siRNA taken up side by side with the biological effect caused by the nucleic acid. For this purpose, we adapted a highly sensitive method for the quantification of siRNA described by Overhoff *et al*. (64) enabling us to detect the antisense-strand of the siRNA with a sensitivity of $\geqslant$10 molecules per cell. This so-called liquid hybridisation assay comprises the extraction of total RNA from the cells and a hybridisation step of a radioactively labelled probe

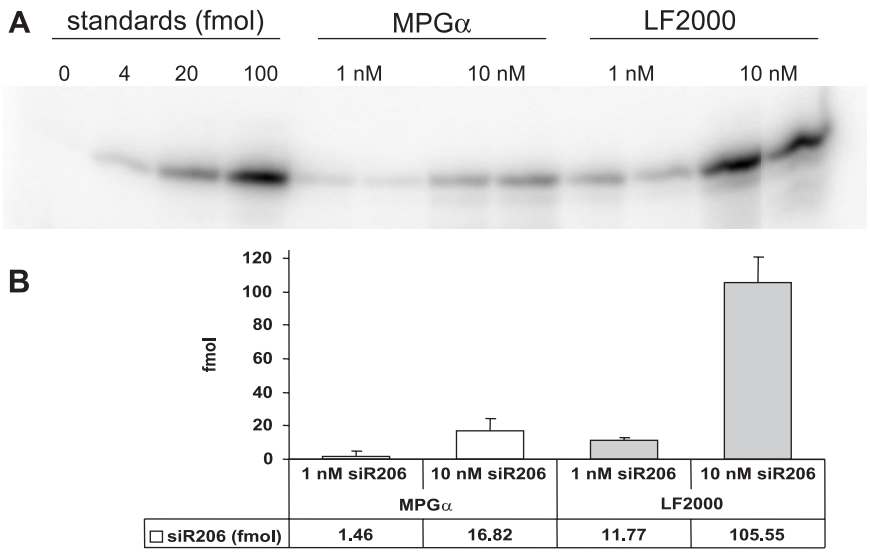

Figure 3. Quantification of the cellular uptake of siRNA after MPGα-mediated delivery. ECV GL3 cells were transfected for 4 h in a 12 well format using 2.1 μM MPGα or 10 μg/ml LF2000 and 1 or 10 nM siR206, respectively. Twenty four hours after transfection, intracellular amounts of siRNA were determined applying the liquid hybridisation protocol as described in the methods section. One representative quantification experiment is shown. (**A**) 20% non-denaturing PAGE analysis of the samples. (**B**) Total amount of siRNA per sample.

with the corresponding antisense-strand of the siRNA in solution. With the help of PAGE analysis the intact portion of intracellular siRNA can be quantified.

Recently, it was convincingly demonstrated by Richard *et al*. (35) that adequate removal of extracellularly bound carrier/cargo complexes is crucial for a correct analysis of intracellular delivery. Taking these findings into account, we examined several washing procedures. For this matter, we quantified the amount of siRNA taken up applying the liquid hybridisation assay and in parallel measured the reduction of the luciferase activity to ensure inhibition reaches the same level as without such a treatment. Additionally, we analysed the cells by fluorescence microscopy. Besides a treatment of the cells with trypsin as suggested by Richard *et al*. (35), we tested heparin and a combination of trypsin and heparin under different conditions (Supplementary Figure 2). By far, the best results were obtained with a heparin wash (15 U/ml, three times totalling one hour at 37°C) reducing the amount of allegedly intracellular siRNA by 60% as compared to a PBS wash of the cells, while a trypsin treatment increased the observed signal by 2-fold in our hands and a combination of both yielded comparable results as heparin alone. The necessity and efficacy of the heparin wash is impressively illustrated by the fluorescence microscopy pictures given in Supplementary Figure 2A. As a result, following the transfection step a heparin wash was included into the protocol, irrespective of further treatments.

Applying this modified setup we performed quantitative measurements with ECV GL3 cells. Figure 3 shows the results of a typical experiment. Here, either 1 or 10 nM siR206 were transfected for 4 h with either MPGα or LF2000 in a 12 well format. After 1 h of heparin treatment and further 19 h of incubation with medium supplemented with 10% FCS the amount of siRNA taken up by the cells was quantified utilising the liquid hybridisation assay. In total, 16.8 fmol siR206 were detectable after transfection of 10 nM siR206 with the peptide as compared to 105.5 fmol after transfection with LF2000. Reducing the extracellular concentration of nucleic acid cargo by 10-fold, we observed a corresponding reduction in uptake by 10-fold. Further experiments revealed that uptake was linear between 0.1 nM and 100 nM siRNA in the transfection mix for both transfection reagents (data not shown). Table 2 summarises a set of data from six independent uptake experiments (including the results shown in Figure 3). Quantification via liquid hybridisation was performed 4 or 24 h after transfection with either reagent. With the peptide ~3% of the siRNA present in the initial transfection mixture was detected inside the cells after 4 h plus 1 h of heparin treatment. After 24 h this value had dropped to ca. 0.7%. During the first 4 h of incubation LF2000 delivered twice as much siRNA as MPGα. After 24 h the amount of intracellular siRNA exceeded that measured for MPGα-mediated transfection by a factor of 4–6. However, at half maximal inhibition of reporter gene activity 10 000 siRNA molecules were detected inside the cells in case of MPGα-mediated delivery, whereas in case of LF2000 only 300 molecules per cell were measured. Thus, the amount of bio-available siRNA molecules inside the cells was about 30-fold lower for peptide-mediated delivery as compared to cationic lipid-mediated delivery.

Insights into the mechanism of MPGα-mediated delivery of siRNAs

As outlined above, quantification of siRNA delivered into mammalian cells either by LF2000 or MPGα revealed a considerable difference in the absolute amount of molecules required to trigger an equivalent inhibitory effect. Hence, we strived for a closer look at the fate of carrier/cargo complexes inside the cells by applying fluorescence microscopy. All microscopic images shown in this study were obtained with unfixed living cells. This is particularly important with

Table 2. Quantification of MPGα- and LF2000-mediated delivery of siRNA

Incubation prior to quantification (h)	Delivery agent	siRNA (fmol) detected per µg of total cellular RNA	siRNA detected inside of applied outside (%)	siRNA per cell (amol)	Molecules per cell × 10^5
4	LF2000	10.8 (±5.7)	4.2 (±2.4)	0.28 (±0.16)	1.66 (±0.94)
24	LF2000	6.3 (±3.4)	2.9 (±1.4)	0.18 (±0.10)	1.05 (±0.62)
4	MPGα	8.6 (±5.1)	2.8 (±1.6)	0.18 (±0.10)	1.06 (±0.55)
24	MPGα	1.6 (±1.3)	0.7 (±0.5)	0.05 (±0.03)	0.27 (±0.19)

The table shows averaged data of six independent experiments. For better comparison of different experimental conditions the results were normalised to a transfection of 1 pmol siRNA with either 2.1 µM MPGα or 10 µg/ml LF2000 in a 12 well format. Quantification via the liquid hybridisation protocol was performed after 4 or 24 h as described in the methods section. Molecules per cell were calculated on the basis of the cell number seeded for transfection.

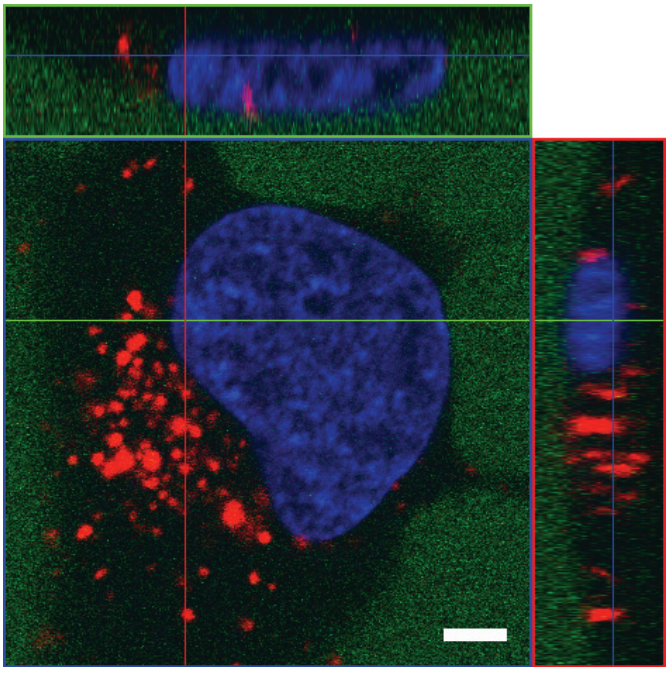

Figure 4. Confocal laser scanning microscopy analysis of unfixed HeLa cells after transfection with MPGα/RNA complexes. Cells were transfected for 3 h with complexes of 5 µM peptide and 180 nM Cy3-labelled RNA in OptiMEM. Adding free carboxyfluorescein to the medium leads to a green staining of the extracellular space. The red and the green lines show the position within the image of the projections given in the upper and right part, respectively. Microscopical analysis was performed with a confocal laser scanning microscope (LSM 510, Carl Zeiss). The white bar equals 10 µm.

respect to earlier publications (35), which had demonstrated that cell fixation procedures can lead to localisation artefacts of cargo and carrier inside the cell. Microscopic studies were performed with unlabelled MPGα peptide and fluorescently labelled oligonucleotides. To exclude any artefacts, which might arise from the fluorescence label, we compared different fluorophores. Experiments with Cy3 and Alexa^{488} labels at different positions of the nucleic acid cargo gave interchangeable results (data not shown). Figure 4 shows a typical uptake experiment analysed by confocal laser scanning microscopy with a punctual non-homogeneous distribution pattern of the nucleic acid inside the cell indicative of an endocytotic uptake mechanism. The addition of carboxyfluorescein to the medium facilitates a discrimination of the non-fluorescent cytoplasm from the green fluorescent extracellular space. This easily allows for a differentiation of complexes attached to the cellular surface and complexes internalised into the cells. Furthermore, as can be seen on the projections in Figure 4 and when zooming through the image (data not provided) the vast majority of red dots visible are indeed inside the observed cell.

Next, we analysed the influence of specific inhibitors/effectors of different endocytotic pathways on the delivery of siRNA and in parallel on the inhibition of reporter gene activity. The compounds used in this study are summarised in Table 1. Additionally, a brief description of the proposed mode of action is given for each substance. In general, these inhibitors/effectors of endocytosis exert a high level of stress on the cells, so one has to carefully define the concentration range, which can be applied with maximal effect but minimal toxicity. To find out suitable conditions for the particular cell lines used here, cytotoxicity studies were performed (data not shown). The impact of the substances on siRNA-mediated down-regulation of luciferase activity after peptide-mediated delivery was measured at an extracellular concentration of 1 nM siR206, i.e. in the range of the IC_{50} value (see above), since under these conditions a maximal effect would be expected. For transfections with LF2000 a concentration of 0.1 nM siRNA was applied.

The strongest inhibitory effect on RNAi was observed when transfections were performed at 4°C. Here, uptake was drastically reduced and no RNAi could be detected anymore (Figure 5A and B) clearly indicating an energy-driven cellular process to be responsible for the uptake of the complexes. The inhibitors/effectors sucrose, cytochalasin B, nystatin, wortmannin and okadaic acid reduced siRNA-mediated down-regulation of luciferase activity whereas filipin complex, monensin and especially chloroquine enhanced RNAi efficiency. These data provided additional evidences for endocytotic processes and for the involvement of acidic compartments in the uptake mechanism of MPGα/siRNA complexes. Apart from low temperature, only the application of wortmannin and filipin complex resulted in reduced uptake of siRNA both after 4 and 24 h. Chloroquine slightly increased uptake when measured after 4 h. However, no difference could be observed after 24 h versus transfections without this compound. This is probably due to the fact, that chloroquine promotes the release of nucleic acids from endosomal compartments, which leads to higher amounts of siRNA detected during the first hours. Upon treatment with nystatin, the uptake was significantly increased after 4 h of incubation with even higher values reached after 24 h. Treatment with okadaic acid led to enhanced uptake after 4 h and slightly reduced uptake after 24 h as compared to untreated cells.

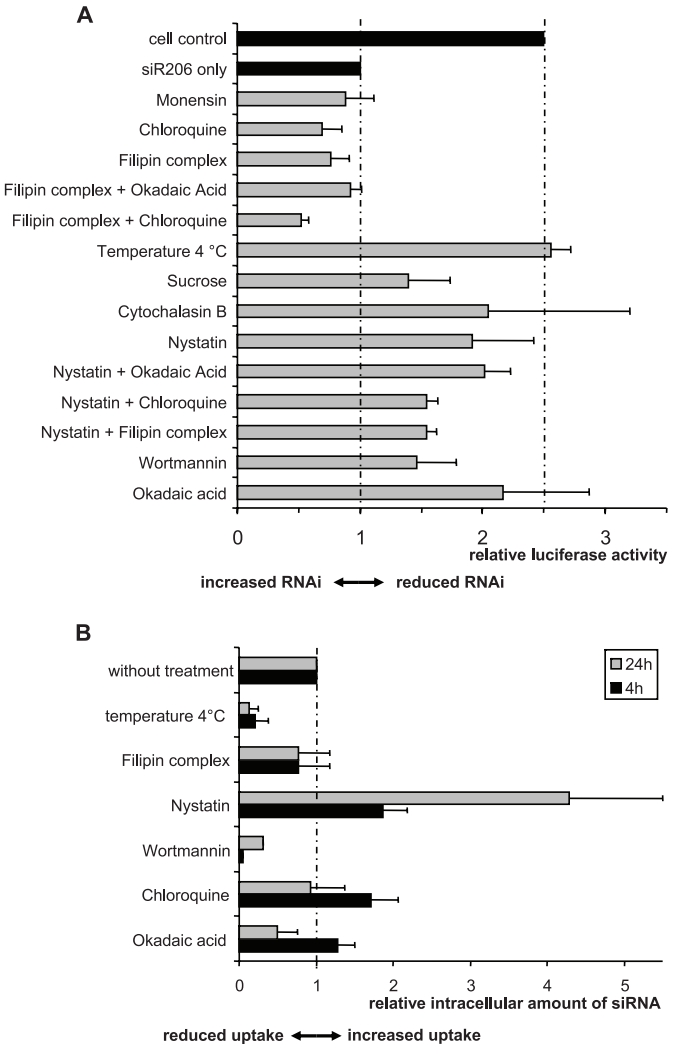

Figure 5. RNAi efficiency (**A**) and intracellular amounts of siRNA (**B**) after MPGα-mediated delivery in the presence of inhibitors/effectors of endocytosis. Prior to a 4 h transfection with complexes of 2.1 μM MPGα and 1 nM siR206, ECV GL3 cells were pre-incubated for 1 h with different modulators of endocytosis at concentrations given in Table 1. The agents were present during the entire experiment. Additionally, transfections were performed at 4°C. The data shown are averages of at least three independent experiments. (A) RNAi efficiency expressed as relative luciferase activity was measured 24 h after transfection in a 96 well format. (B) Uptake of siRNA was analysed 4 or 24 h after transfection in a 12 well format using the liquid hybridisation protocol. The dashed lines show the situation without treatment.

For LF2000, we found a slightly different pattern for the RNAi effect and siRNA uptake in the presence of these agents, which nevertheless corroborated the notion that LF2000/siRNA complexes are taken up by endocytosis (Supplementary Figure 4).

In an attempt to find out the minimal number of siRNA molecules needed to trigger RNAi-mediated half maximal inhibition of luciferase activity we performed nuclear microinjection studies of a luciferase expression plasmid together with varying concentrations of siR206 into HeLa, HTOL and ECV304 cells, respectively. From the IC_{50} value it could be calculated that ~300 siRNA molecules per cell were necessary to observe a half maximal inhibition of the luciferase activity (Figure 6).

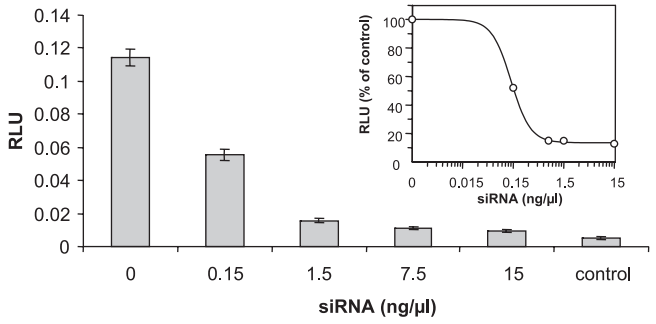

Figure 6. IC_{50} of anti-luciferase siRNA delivered via nuclear microinjection into HeLa-TetOff cells. The plasmid pTRE2hyg-luc (130 ng/μl) was co-injected with varying concentrations (0.0015–15 ng/μl) of siR206 into the nucleus of ~300 cells per experiment. Twenty four hours after microinjection the luciferase activity was analysed. Non-injected cells served as control. The luciferase expression is given as the percentage of active siR206 versus control cells (mean values of two independent microinjection experiments are given). The inset shows a fit of the experimental data using the GraFit5 software yielding an IC_{50} value of 15 ng/μl (±0.49). This value translates into ~300 siRNA molecules per cell.

DISCUSSION

The cell membrane is one of the major barriers for an application of therapeutically interesting bio-macromolecules like nucleic acids. In the present study we exploited a CPP-approach for the delivery of siRNA as a general example for an oligonucleotide cargo using the peptide MPGα, a derivative of the original MPG peptide described by Morris *et al.* (24). MPGα differs from MPG by six amino acids in the hydrophobic part (57). These changes result in an alteration of the overall structure of the peptide towards a higher tendency of adopting a helical conformation (57). The peptide forms stable non-covalent complexes with nucleic acids. Besides the mechanism of cellular uptake of MPGα/siRNA complexes our main focus was a comparative parallel analysis of uptake versus functional effects of the nucleic acid cargo. For this purpose, we used a liquid hybridisation protocol in combination with a simple luciferase reporter system. For comparison, the commercially available cationic lipid LF2000 was included into the study.

As shown in Figure 1, MPGα is capable of translocating siRNA into mammalian cells leading to a down-regulation of the target protein luciferase. The observed effect was highly specific for siR206 and maximal inhibition was achieved with a charge ratio of 15:1, i.e. positive (peptide) over negative (siRNA) charges (Supplementary Figure 1). Additionally, we tested MPGα-mediated delivery of siRNA directed to two other targets, namely ICAM-1 and lamin A/C applying published protocols (58,61). In both cases we observed a substantial RNAi effect of the active siRNA as compared to a control siRNA (data not shown). These data clearly indicate a specific siRNA-mediated inhibition of target protein expression rather than an unspecific effect, which might be caused by the transfection procedure. Comparing the peptide with LF2000, the maximal achievable levels of siRNA-mediated target protein down-regulation are roughly the same. However, an exact determination of the IC_{50} values of both carrier/cargo complexes revealed an ~30-fold lower efficiency of MPGα compared to LF2000. To investigate if this phenomenon was caused by different

levels of uptake or insufficient bio-availability of the siRNA molecules, we quantified the intracellular amount of cargo. From a number of diverse procedures described in the literature (65–68) we adapted a liquid hybridisation protocol described by Overhoff *et al*. (64). This assay does not need any modification of the siRNA and exclusively detects intact molecules. Thus, artefacts due to detached fluorescence labels or degraded cargos for example are precluded. Overall, the liquid hybridisation protocol is a fast, easy to handle and highly reproducible procedure that can be carried out in any laboratory without the need of expensive equipment.

Though, before we could perform quantitative uptake experiments, we had to establish a washing procedure in order to remove complexes bound to the surface of the cells. Such extracellularly attached carrier/cargo complexes are an important source of overestimation of cargo internalised (35). As opposed to the commonly used trypsin treatment, a heparin wash was much more effective in our hands (Supplementary Figure 2A and B). Similar results were reported by Kaplan *et al*. (69) for the cellular uptake of Tat peptide in the absence of cargo. The negatively charged heparin molecules, with a molecular weight of 4–6 kDa, are much smaller than trypsin and thus might be able to infiltrate the extracellular matrix more effectively and both detach and, more importantly, dissociate MPGα/siRNA complexes bound there. In contrast to this, trypsin considerably increased the apparent uptake of the complexes (Supplementary Figure 2B). This might be due to a membrane destabilising effect of this enzyme which has been shown to enhance the uptake of small molecules or oligonucleotides (70). For several CPPs without a cargo it has previously been shown that the cellular penetration is inhibited by certain GAGs suggesting that uptake is mediated by GAG receptors on the cell surface (30,32,56,71). To what extent these receptors are equally involved in the uptake of MPGα/siRNA complexes cannot be answered with certainty as heparin has a very strong destabilising effect on the peptide/nucleic acid complexes (A.T., unpublished data).

With a reliable washing procedure to remove extracellular complexes in place we were able to accurately quantify the intracellular amounts of cargo after carrier-mediated delivery (Figure 3 and Table 2). The amount of siRNA internalised, increased as expected with the incubation time of transfection showing a maximum at ∼4 h (Supplementary Figure 3B and C). Similar results were observed with a RNA aptamer [(72), S.L., unpublished data]. Accordingly, unless otherwise indicated, all transfections were performed for a period of 4 h before cells were either subjected to quantification (after an additional 1 h heparin wash) or further incubated in the absence of carrier/cargo complexes for later analyses. After 24 h approximately half of the maximal amount of siRNA internalised was still detectable. All in all <5% of the siRNA present in the initial transfection mixture was internalised into the cells regardless of the delivery agent. After 4 h, twice as much siRNA was detected inside the cells after transfection with LF2000 when compared to MPGα-mediated delivery. Surprisingly, 24 h after transfection this difference rose to a factor of 4–6. *In vitro* experiments, on the other hand, show that siRNA complexed with the carrier peptide is strongly protected from degradation (data not shown). The observed uptake of siRNA was linear over a tested range of 0.1–100 nM of siRNA. We deliberately did not apply concentrations >100 nM siRNA to examine if the process would eventually be saturable, since too high concentrations of siRNA lead to off-target effects (73,74). Taken together, the difference in uptake between the peptide and the cationic lipid was much smaller than anticipated from the above described IC_{50} values with a factor of about 2–6 in favor of LF2000. These findings clearly indicate that uptake *per se* was not the limiting factor of the peptide approach. Combining both techniques, the analysis of uptake and RNAi effect, it became apparent that for a half maximal inhibition of reporter gene activity, ∼10 000 siRNA molecules were necessary in case of MPGα-mediated delivery, whereas in case of LF2000 only ∼300 molecules were required. Thus, the amount of bio-available siRNA molecules inside the cells was about 30-fold lower for peptide-mediated delivery as compared to cationic lipid-mediated delivery. To the best of our knowledge, this is the first time the number of siRNA molecules per cell has been determined for half maximal inhibition of the target for peptide- versus cationic lipid-mediated delivery. At this point the question arose, what the cause of this observed discrepancy was. An obvious reason for these findings would be a difference in the mechanism of uptake. As outlined above, the mechanisms underlying the cellular translocation of CPPs are poorly understood and remain hotly debated. Nonetheless, there is considerable evidence that endocytosis is a major route of the internalisation of many CPPs. In an attempt to address this question we performed fluorescence microscopy studies and analysed the influence of specific inhibitors/effectors of different endocytotic pathways on the delivery of siRNA and the inhibition of reporter gene activity simultaneously.

A first clear hint for an endocytotic pathway involved in the uptake of MPGα/siRNA complexes arose from microscopy studies (Figure 4). Consistent with the assumption of an endocytotic pathway, a typical vesicular distribution pattern in the cytoplasm could be observed by fluorescence microscopy. Moreover, the siRNA internalised was observed to partially co-localise with endosomal/lysosomal compartments (data not shown). The results were very similar for LF2000-mediated transfection though here a slight diffuse distribution of fluorescence throughout the cytoplasm was recognisable but hard to document. To avoid any artefacts due to cell fixation, all fluorescence microscopy experiments were performed with living cells. The heparin wash described above proved to be essential as images of cells not treated with heparin showed large aggregates on the cell surface impairing the view on complexes internalised (as clearly seen in Supplementary Figure 2A). Addition of trypan blue to quench external fluorescence (32,75) was only suitable for smaller complexes but larger ones remained visible. Carboxyfluorescein in the medium turned out to be very useful to distinguish between the inside and the outside of the cell and was used to clearly discriminate between intra- and extracellular complexes. Although MPGα harbors an NLS sequence, no nuclear localisation could be observed nor was there any change in the apparent RNAi effect when the NLS sequence was mutated (data not shown). On the other hand, it cannot be ruled out that the amount of cargo localised in the nucleus was below the detection limit. According to a recent study of Berezhna *et al*. (76) the intracellular localisation of

siRNA is suggested to depend on the localisation of the target. Nonetheless, applying a fluorescently labeled siRNA against the 7SK RNA, which was shown to strictly localise in the nucleus (77–80), we did not observe any fluorescence there (data not shown).

Lowering of the temperature markedly reduces flexibility and fluidity of the plasma membrane, thereby also slowing membrane traffic (81) and blocking all endocytotic processes (82). Consistent with this concept, we could neither detect MPGα-mediated siRNA delivery at 4°C as shown by liquid hybridisation analyses as well as by fluorescence microscopy (Supplementary Figure 3), nor did we observe any RNAi effect (Figure 5). In accordance with our findings, other authors also suggested an energy-dependent uptake process for CPP-mediated delivery based on the observation that uptake was strongly decreased at low temperatures (31,83,84). In order to address this issue in more detail, we performed studies on MPGα with different modulators of endocytosis (Figure 5). First we analysed the effect of wortmannin, a compound, which is supposed to affect clathrin-dependent endocytosis (85) and macropinocytosis (86). Wortmannin led to a strong reduction in the uptake of MPGα/siRNA complexes. Like with sucrose, which also blocks clathrin-dependent endocytosis unselectively, the RNAi effect was reduced significantly. On the other hand, no clear-cut influence on uptake of siRNA could be seen applying cytochalasin B, which is supposed to affect the assembly of actin microfilaments (87,88), whereas the RNAi effect was strongly diminished in the presence of this compound. Hence, we could not distinguish, whether this was due to a blockage of macropinocytosis or what appears more realistic was caused by a block of intracellular vesicle transport. In the presence of nystatin, which is supposed to inhibit caveolin-dependent lipid-raft-mediated endocytosis (89,90), the RNAi effect was clearly reduced and could neither be rescued by combining nystatin with okadaic acid, chloroquine nor filipin complex (Figure 5A). Pre-incubation of the cells with nystatin led to an increase in uptake during the first 4 h, which was even more pronounced when the quantification was performed after 24 h (Figure 5B). An additional effect of nystatin is supposed to be an increase in cell membrane permeability (89). This property of nystatin could account for the high amount of siRNA taken up. Together with the reduced RNAi effect observed, this would mean that nucleic acids internalised this way, are not available for the RNAi machinery. Then again, taking the results of experiments into account in which different inhibitors were combined to counteract nystatin, it could be concluded that nystatin itself had a severe negative effect on the RNAi machinery. Filipin complex like nystatin shows sterol-binding properties (91–93). However, in contrast to nystatin almost no change in siRNA uptake was detected after MPGα-mediated delivery, whereas the RNAi effect was slightly increased. This may be due to a selective inhibition of caveolin-mediated endocytosis, which in turn might shift the balance towards clathrin-mediated endocytosis. This interpretation would be consistent with our idea that clathrin-mediated endocytosis yields more bio-available cargo and is further supported by the observation that the RNAi effect is increased even more by combining filipin complex with chloroquine (Figure 5A). Okadaic acid, a specific phosphatase inhibitor, is supposed to stimulate mobility and internalization of caveolae (94–96). In the presence of okadaic acid no RNAi effect could be detected. Uptake of siRNA, on the other hand, was not affected. This could be interpreted as an increase of caveolin-dependent endocytosis accompanied by a reduction of clathrin-dependent uptake leading to an unchanged net amount of intracellular siRNA. Caveolae direct most of their cargo via caveosomes to the Golgi apparatus where they are probably beyond reach of the RNAi machinery. In addition, combining filipin complex and okadaic acid resulted in levels of luciferase activity equal to those measured with siRNA alone. Here, induction of caveolin-mediated endocytosis by okadaic acid was possibly compensated by the inhibitory effect of filipin complex. Chloroquine, a weak base, is supposed to prevent lysosomal degradation by inhibiting the acidification of endosomes (97,98). This eventually leads to the disruption of a large portion of the endosomes which then release their content into the cytoplasm (99). In our hands, chloroquine caused a slightly enhanced RNAi effect leading to the conclusion that an increased number of siRNA molecules have become bio-available by endosomal release.

Equivalent experiments with LF2000 as transfection reagent yielded a slightly different pattern, for example regarding uptake in the presence of nystatin or chloroquine, nevertheless strongly indicating uptake via endocytosis (Supplementary Figure 4). This observation is consistent with the findings of others concerning the uptake mechanism of several cationic lipids (100–102).

Overall, our data, especially those addressing the temperature-dependency of the uptake, strongly indicate that both MPGα and LF2000/siRNA complexes are taken up by endocytotic processes. The differences between transfections with MPGα and LF2000 concerning the IC_{50} values of siRNA could be explained by the property of LF2000 to promote endosomal escape at least partially, which is consistent with the microscopic observations described above. The somewhat controversial results concerning different inhibitors of endocytosis described above support the notion that not one single pathway is responsible for the uptake of the complexes but rather several pathways are involved. This may be due to a relatively unspecific interaction of the complexes with numerous negatively charged molecules on the cell surface. As a result, various pathways of endocytosis might be triggered. Accordingly, individual inhibitors used in this study might show just moderate effects by shifting the balance in favour of a particular endocytotic pathway. Analogous results were reported by Säälik *et al*. for CPP/avidin complexes (103). However, it should be kept in mind, that the interpretation of these particular experimental data is problematic, as many aspects of endocytosis are still poorly understood to date. Even more important, the compounds may have additional unknown effects, which could lead to unexpected changes in reporter gene activity and/or affect the RNAi machinery. Besides, the involvement of several pathways of endocytosis could also be a direct result of an inhomogeneous size distribution of the MPGα/siRNA complexes (S.V. and A.T., unpublished data), since for each process only a certain range of particle sizes is believed to be predominantly taken up (50,104,105). Thus, the size of the complexes may determine their uptake route and consequently their fate. Then again, we cannot entirely rule out

that a certain percentage of complexes are taken up via a direct penetration of the plasma membrane as reported by others (39,40,42). In this context it would be very interesting to know the minimal number of siRNA molecules needed to trigger RNAi-mediated half maximal inhibition of luciferase activity. In an attempt to answer this question, we performed technically challenging nuclear microinjection studies of a luciferase expression plasmid together with siR206 into HeLa and ECV304 cells, respectively (Figure 6). From such experiments it could be calculated that ~300 siRNA molecules per cell were necessary to observe a half maximal inhibition of luciferase activity. Surprisingly, this number is very close to what was determined for LF2000-mediated delivery. Microscopic studies of fluorescently labelled siRNA delivered with LF2000 on the other hand, showed a vesicular distribution similar to what has been observed with MPGα, indicative of the majority of siRNA molecules being not bio-available either (Supplementary Figure 5). Thus, the microinjection approach, at least in our hands, turned out not to be practicable to answer this question. A possible cause could simply be that the siRNA is retained inside the nucleus. Then again, this could not be verified by microinjection of fluorescently labelled siRNA as initially strongly visible fluorescence in the nucleus completely disappeared within 30 min, probably either due to quenching effects or transport into cytoplasm. In spite of this, transiently transfected cells might differ considerably from stably transfected ones.

In conclusion, our data clearly show that a vesicular (presumably endosomal) accumulation of the cargo and not uptake *per se* is the bottleneck of MPGα-mediated RNA delivery rendering the vast majority of intracellular siRNA cargo molecules inactive. Thus, like for other non-viral delivery systems, solving the problem of vesicular escape remains the main challenge for this CPP approach. Nonetheless, this approach yields IC_{50} values for siRNA delivery in the sub-nanomolar range far superior to other CPP systems together with the advantage of non-covalent complex formation. Moreover, this study describes a combination of techniques which represent easy to handle tools suitable for a detailed analysis of carrier-mediated delivery of therapeutically interesting nucleic acid molecules, which eventually may lead to considerably improved delivery.

SUPPLEMENTARY DATA

Supplementary Data are available at NAR online.

ACKNOWLEDGEMENTS

We thank Andreas Gebert for his help with the confocal laser scanning microscope, Laurent Chaloin, Gilles Divita and Frédéric Heitz for their help and advice during initial stages of the project, Rosel Kretschmer-Kazemi Far and Marita Overhoff for materials and technical advice and Christian Tscheik for his contribution to Supplementary Figure 4. T.R. acknowledges funding by EC-grants QLK2-2001-01451 and LSHG-CT-2003-503480. Funding to pay the Open Access publication charges for this article was provided by EC-grant LSHG-CT-2003-503480.

Conflict of interest statement. None declared.

REFERENCES

1. Opalinska,J.B. and Gewirtz,A.M. (2002) Nucleic-acid therapeutics: basic principles and recent applications. *Nature Rev. Drug Discov.*, **1**, 503–514.
2. Verma,I.M. and Weitzman,M.D. (2005) Gene therapy: twenty-first century medicine. *Annu. Rev. Biochem.*, **74**, 711–738.
3. Kootstra,N.A. and Verma,I.M. (2003) Gene therapy with viral vectors. *Annu. Rev. Pharmacol. Toxicol.*, **43**, 413–439.
4. Hacein-Bey-Abina,S., Von Kalle,C., Schmidt,M., McCormack,M.P., Wulffraat,N., Leboulch,P., Lim,A., Osborne,C.S., Pawliuk,R., Morillon,E. *et al.* (2003) LMO2-associated clonal T cell proliferation in two patients after gene therapy for SCID-X1. *Science*, **302**, 415–419.
5. Raper,S.E., Chirmule,N., Lee,F.S., Wivel,N.A., Bagg,A., Gao,G.P., Wilson,J.M. and Batshaw,M.L. (2003) Fatal systemic inflammatory response syndrome in a ornithine transcarbamylase deficient patient following adenoviral gene transfer. *Mol. Genet. Metab.*, **80**, 148–158.
6. Check,E. (2005) Gene therapy put on hold as third child develops cancer. *Nature*, **433**, 561.
7. Sorensen,D.R., Leirdal,M. and Sioud,M. (2003) Gene silencing by systemic delivery of synthetic siRNAs in adult mice. *J. Mol. Biol.*, **327**, 761–766.
8. Chien,P.Y., Wang,J., Carbonaro,D., Lei,S., Miller,B., Sheikh,S., Ali,S.M., Ahmad,M.U. and Ahmad,I. (2005) Novel cationic cardiolipin analogue-based liposome for efficient DNA and small interfering RNA delivery *in vitro* and *in vivo*. *Cancer Gene Ther.*, **12**, 321–328.
9. Minakuchi,Y., Takeshita,F., Kosaka,N., Sasaki,H., Yamamoto,Y., Kouno,M., Honma,K., Nagahara,S., Hanai,K., Sano,A. *et al.* (2004) Atelocollagen-mediated synthetic small interfering RNA delivery for effective gene silencing *in vitro* and *in vivo*. *Nucleic Acids Res.*, **32**, e109.
10. Takeshita,F., Minakuchi,Y., Nagahara,S., Honma,K., Sasaki,H., Hirai,K., Teratani,T., Namatame,N., Yamamoto,Y., Hanai,K. *et al.* (2005) Efficient delivery of small interfering RNA to bone-metastatic tumors by using atelocollagen *in vivo*. *Proc. Natl Acad. Sci. USA*, **102**, 12177–12182.
11. Urban-Klein,B., Werth,S., Abuharbeid,S., Czubayko,F. and Aigner,A. (2005) RNAi-mediated gene-targeting through systemic application of polyethylenimine (PEI)-complexed siRNA *in vivo*. *Gene Ther.*, **12**, 461–466.
12. Grzelinski,M., Urban-Klein,B., Martens,T., Lamszus,K., Bakowsky,U., Hobel,S., Czubayko,F. and Aigner,A. (2006) RNA interference-mediated gene silencing of pleiotrophin through polyethylenimine-complexed small interfering RNAs *in vivo* exerts antitumoral effects in glioblastoma xenografts. *Hum. Gene Ther.*, **17**, 751–766.
13. Soutschek,J., Akinc,A., Bramlage,B., Charisse,K., Constien,R., Donoghue,M., Elbashir,S., Geick,A., Hadwiger,P., Harborth,J. *et al.* (2004) Therapeutic silencing of an endogenous gene by systemic administration of modified siRNAs. *Nature*, **432**, 173–178.
14. Zimmermann,T.S., Lee,A.C., Akinc,A., Bramlage,B., Bumcrot,D., Fedoruk,M.N., Harborth,J., Heyes,J.A., Jeffs,L.B., John,M. *et al.* (2006) RNAi-mediated gene silencing in non-human primates. *Nature*, **441**, 111–114.
15. Green,M. and Loewenstein,P.M. (1988) Autonomous functional domains of chemically synthesized human immunodeficiency virus tat trans-activator protein. *Cell*, **55**, 1179–1188.
16. Frankel,A.D. and Pabo,C.O. (1988) Cellular uptake of the tat protein from human immunodeficiency virus. *Cell*, **55**, 1189–1193.
17. Joliot,A.H., Triller,A., Volovitch,M., Pernelle,C. and Prochiantz,A. (1991) alpha-2,8-Polysialic acid is the neuronal surface receptor of antennapedia homeobox peptide. *New Biol.*, **3**, 1121–1134.
18. Fawell,S., Seery,J., Daikh,Y., Moore,C., Chen,L.L., Pepinsky,B. and Barsoum,J. (1994) Tat-mediated delivery of heterologous proteins into cells. *Proc. Natl Acad. Sci. USA*, **91**, 664–668.
19. Allinquant,B., Hantraye,P., Mailleux,P., Moya,K., Bouillot,C. and Prochiantz,A. (1995) Downregulation of amyloid precursor protein inhibits neurite outgrowth *in vitro*. *J. Cell Biol.*, **128**, 919–927.
20. Schwarze,S.R. and Dowdy,S.F. (2000) *In vivo* protein transduction: intracellular delivery of biologically active proteins, compounds and DNA. *Trends Pharmacol. Sci.*, **21**, 45–48.

21. Dietz,G.P. and Bahr,M. (2004) Delivery of bioactive molecules into the cell: the Trojan horse approach. *Mol. Cell Neurosci.*, **27**, 85–131.
22. Fischer,R., Fotin-Mleczek,M., Hufnagel,H. and Brock,R. (2005) Break on through to the other side-biophysics and cell biology shed light on cell-penetrating peptides. *Chembiochem.*, **6**, 2126–2142.
23. Zatsepin,T.S., Turner,J.J., Oretskaya,T.S. and Gait,M.J. (2005) Conjugates of oligonucleotides and analogues with cell penetrating peptides as gene silencing agents. *Curr. Pharm. Des.*, **11**, 3639–3654.
24. Morris,M.C., Vidal,P., Chaloin,L., Heitz,F. and Divita,G. (1997) A new peptide vector for efficient delivery of oligonucleotides into mammalian cells. *Nucleic Acids Res.*, **25**, 2730–2736.
25. Morris,M.C., Depollier,J., Mery,J., Heitz,F. and Divita,G. (2001) A peptide carrier for the delivery of biologically active proteins into mammalian cells. *Nat. Biotechnol.*, **19**, 1173–1176.
26. Morris,M.C., Chaloin,L., Heitz,F. and Divita,G. (2000) Translocating peptides and proteins and their use for gene delivery. *Curr. Opin. Biotechnol.*, **11**, 461–466.
27. Rusnati,M., Coltrini,D., Oreste,P., Zoppetti,G., Albini,A., Noonan,D., d'Adda,D.F., Giacca,M. and Presta,M. (1997) Interaction of HIV-1 Tat protein with heparin. Role of the backbone structure, sulfation, and size. *J. Biol. Chem.*, **272**, 11313–11320.
28. Rusnati,M., Tulipano,G., Spillmann,D., Tanghetti,E., Oreste,P., Zoppetti,G., Giacca,M. and Presta,M. (1999) Multiple interactions of HIV-I Tat protein with size-defined heparin oligosaccharides. *J. Biol. Chem.*, **274**, 28198–28205.
29. Tyagi,M., Rusnati,M., Presta,M. and Giacca,M. (2001) Internalization of HIV-1 tat requires cell surface heparan sulfate proteoglycans. *J. Biol. Chem.*, **276**, 3254–3261.
30. Suzuki,T., Futaki,S., Niwa,M., Tanaka,S., Ueda,K. and Sugiura,Y. (2002) Possible existence of common internalization mechanisms among arginine-rich peptides. *J. Biol. Chem.*, **277**, 2437–2443.
31. Console,S., Marty,C., Garcia-Echeverria,C., Schwendener,R. and Ballmer-Hofer,K. (2003) Antennapedia and HIV transactivator of transcription (TAT) 'protein transduction domains' promote endocytosis of high molecular weight cargo upon binding to cell surface glycosaminoglycans. *J. Biol. Chem.*, **278**, 35109–35114.
32. Foerg,C., Ziegler,U., Fernandez-Carneado,J., Giralt,E., Rennert,R., Beck-Sickinger,A.G. and Merkle,H.P. (2005) Decoding the entry of two novel cell-penetrating peptides in HeLa cells: lipid raft-mediated endocytosis and endosomal escape. *Biochemistry*, **44**, 72–81.
33. Mano,M., Teodosio,C., Paiva,A., Simoes,S. and Pedroso de Lima,M.C. (2005) On the mechanisms of the internalization of S4(13)-PV cell-penetrating peptide. *Biochem. J.*, **390**, 603–612.
34. Astriab-Fisher,A., Sergueev,D., Fisher,M., Shaw,B.R. and Juliano,R.L. (2002) Conjugates of antisense oligonucleotides with the Tat and antennapedia cell-penetrating peptides: effects on cellular uptake, binding to target sequences, and biologic actions. *Pharm. Res.*, **19**, 744–754.
35. Richard,J.P., Melikov,K., Vives,E., Ramos,C., Verbeure,B., Gait,M.J., Chernomordik,L.V. and Lebleu,B. (2003) Cell-penetrating peptides. A reevaluation of the mechanism of cellular uptake. *J. Biol. Chem.*, **278**, 585–590.
36. Barany-Wallje,E., Keller,S., Serowy,S., Geibel,S., Pohl,P., Bienert,M. and Dathe,M. (2005) A critical reassessment of penetratin translocation across lipid membranes. *Biophys. J.*, **89**, 2513–2521.
37. Turner,J.J., Arzumanov,A.A. and Gait,M.J. (2005) Synthesis, cellular uptake and HIV-1 Tat-dependent trans-activation inhibition activity of oligonucleotide analogues disulphide-conjugated to cell-penetrating peptides. *Nucleic Acids Res.*, **33**, 27–42.
38. Abes,S., Williams,D., Prevot,P., Thierry,A., Gait,M.J. and Lebleu,B. (2006) Endosome trapping limits the efficiency of splicing correction by PNA-oligolysine conjugates. *J. Control Release*, **110**, 595–604.
39. Simeoni,F., Morris,M.C., Heitz,F. and Divita,G. (2003) Insight into the mechanism of the peptide-based gene delivery system MPG: implications for delivery of siRNA into mammalian cells. *Nucleic Acids Res.*, **31**, 2717–2724.
40. Deshayes,S., Gerbal-Chaloin,S., Morris,M.C., Aldrian-Herrada,G., Charnet,P., Divita,G. and Heitz,F. (2004) On the mechanism of non-endosomial peptide-mediated cellular delivery of nucleic acids. *Biochim. Biophys. Acta*, **1667**, 141–147.
41. Thoren,P.E., Persson,D., Esbjorner,E.K., Goksor,M., Lincoln,P. and Norden,B. (2004) Membrane binding and translocation of cell-penetrating peptides. *Biochemistry*, **43**, 3471–3489.
42. Henriques,S.T., Costa,J. and Castanho,M.A. (2005) Translocation of beta-galactosidase mediated by the cell-penetrating peptide pep-1 into lipid vesicles and human HeLa cells is driven by membrane electrostatic potential. *Biochemistry*, **44**, 10189–10198.
43. Thoren,P.E., Persson,D., Lincoln,P. and Norden,B. (2005) Membrane destabilizing properties of cell-penetrating peptides. *Biophys. Chem.*, **114**, 169–179.
44. Tripathi,S., Chaubey,B., Ganguly,S., Harris,D., Casale,R.A. and Pandey,V.N. (2005) Anti-HIV-1 activity of anti-TAR polyamide nucleic acid conjugated with various membrane transducing peptides. *Nucleic Acids Res.*, **33**, 4345–4356.
45. Turner,J.J., Ivanova,G.D., Verbeure,B., Williams,D., Arzumanov,A.A., Abes,S., Lebleu,B. and Gait,M.J. (2005) Cell-penetrating peptide conjugates of peptide nucleic acids (PNA) as inhibitors of HIV-1 Tat-dependent trans-activation in cells. *Nucleic Acids Res.*, **33**, 6837–6849.
46. Pooga,M., Hällbrink,M., Zorko,M. and Langel,Ü. (1998) Cell penetration by transportan. *FASEB J.*, **12**, 67–77.
47. Hällbrink,M., Floren,A., Elmquist,A., Pooga,M., Bartfai,T. and Langel,Ü. (2001) Cargo delivery kinetics of cell-penetrating peptides. *Biochim. Biophys. Acta*, **1515**, 101–109.
48. El Andaloussi,S., Johansson,H., Magnusdottir,A., Järver,P., Lundberg,P. and Langel,Ü. (2005) TP10, a delivery vector for decoy oligonucleotides targeting the Myc protein. *J. Control Release*, **110**, 189–201.
49. Mano,M., Henriques,A., Paiva,A., Prieto,M., Gavilanes,F., Simoes,S. and Pedroso de Lima,M.C. (2006) Cellular uptake of S413-PV peptide occurs upon conformational changes induced by peptide-membrane interactions. *Biochim. Biophys. Acta*, **1758**, 336–346.
50. Conner,S.D. and Schmid,S.L. (2003) Regulated portals of entry into the cell. *Nature*, **422**, 37–44.
51. Le Roy,C. and Wrana,J.L. (2005) Clathrin- and non-clathrin-mediated endocytic regulation of cell signalling. *Nature Rev. Mol. Cell Biol.*, **6**, 112–126.
52. Hellgren,I., Gorman,J. and Sylven,C. (2004) Factors controlling the efficiency of Tat-mediated plasmid DNA transfer. *J. Drug Target*, **12**, 39–47.
53. De Coupade,C., Fittipaldi,A., Chagnas,V., Michel,M., Carlier,S., Tasciotti,E., Darmon,A., Ravel,D., Kearsey,J., Giacca,M. *et al.* (2005) Novel human-derived cell-penetrating peptides for specific subcellular delivery of therapeutic biomolecules. *Biochem. J.*, **390**, 407–418.
54. Maiolo,J.R., Ferrer,M. and Ottinger,E.A. (2005) Effects of cargo molecules on the cellular uptake of arginine-rich cell-penetrating peptides. *Biochim. Biophys. Acta*, **1712**, 161–172.
55. Silhol,M., Tyagi,M., Giacca,M., Lebleu,B. and Vives,E. (2002) Different mechanisms for cellular internalization of the HIV-1 Tat-derived cell penetrating peptide and recombinant proteins fused to Tat. *Eur. J. Biochem.*, **269**, 494–501.
56. Richard,J.P., Melikov,K., Brooks,H., Prevot,P., Lebleu,B. and Chernomordik,L.V. (2005) Cellular uptake of unconjugated TAT peptide involves clathrin-dependent endocytosis and heparan sulfate receptors. *J. Biol. Chem.*, **280**, 15300–15306.
57. Deshayes,S., Plenat,T., Aldrian-Herrada,G., Divita,G., Le Grimellec,C. and Heitz,F. (2004) Primary amphipathic cell-penetrating peptides: structural requirements and interactions with model membranes. *Biochemistry*, **43**, 7698–7706.
58. Kretschmer-Kazemi,F.R. and Sczakiel,G. (2003) The activity of siRNA in mammalian cells is related to structural target accessibility: a comparison with antisense oligonucleotides. *Nucleic Acids Res.*, **31**, 4417–4424.
59. Reynolds,A., Leake,D., Boese,Q., Scaringe,S., Marshall,W.S. and Khvorova,A. (2004) Rational siRNA design for RNA interference. *Nat. Biotechnol.*, **22**, 326–330.
60. Elbashir,S.M., Harborth,J., Lendeckel,W., Yalcin,A., Weber,K. and Tuschl,T. (2001) Duplexes of 21-nucleotide RNAs mediate RNA interference in cultured mammalian cells. *Nature*, **411**, 494–498.
61. Elbashir,S.M., Harborth,J., Weber,K. and Tuschl,T. (2002) Analysis of gene function in somatic mammalian cells using small interfering RNAs. *Methods*, **26**, 199–213.
62. Jarmy,G., Heinkelein,M., Weissbrich,B., Jassoy,C. and Rethwilm,A. (2001) Phenotypic analysis of the sensitivity of HIV-1 to inhibitors of the reverse transcriptase, protease, and integrase using a self-inactivating virus vector system. *J. Med. Virol.*, **64**, 223–231.

63. Jones,K.H. and Senft,J.A. (1985) An improved method to determine cell viability by simultaneous staining with fluorescein diacetate-propidium iodide. *J. Histochem. Cytochem.*, **33**, 77–79.
64. Overhoff,M., Wünsche,W. and Sczakiel,G. (2004) Quantitative detection of siRNA and single-stranded oligonucleotides: relationship between uptake and biological activity of siRNA. *Nucleic Acids Res.*, **32**, e170.
65. Lindgren,M., Hällbrink,M. and Langel,Ü. (2002) Quantification of cell-penetrating peptides and their cargoes. In Langel,Ü. (ed.), *Cell-Penetrating Peptides—Processes and Applications.* CRC Press, Boca Raton, FL, pp. 263–275.
66. Burlina,F., Sagan,S., Bolbach,G. and Chasssaing,G. (2005) Quantification of the cellular uptake of cell-penetrating peptides by MALDI-TOF mass spectrometry. *Angew. Chem. Int. Ed*, **44**, 4244–4247.
67. Jiang,M., Arzumanov,A.A., Gait,M.J. and Milner,J. (2005) A bi-functional siRNA construct induces RNA interference and also primes PCR amplification for its own quantification. *Nucleic Acids Res.*, **33**, e151.
68. Oehlke,J., Lorenz,D., Wiesner,B. and Bienert,M. (2005) Studies on the cellular uptake of substance P and lysine-rich, KLA-derived model peptides. *J. Mol. Recognit.*, **18**, 50–59.
69. Kaplan,I.M., Wadia,J.S. and Dowdy,S.F. (2005) Cationic TAT peptide transduction domain enters cells by macropinocytosis. *J. Control Release*, **102**, 247–253.
70. Lamb,J.F. and Ogden,P.H. (1987) Transient changes in permeability in HeLa and L cells during detachment from a substrate. *Q. J. Exp. Physiol.*, **72**, 189–199.
71. Wadia,J.S., Stan,R.V. and Dowdy,S.F. (2004) Transducible TAT-HA fusogenic peptide enhances escape of TAT-fusion proteins after lipid raft macropinocytosis. *Nature Med.*, **10**, 310–315.
72. Kensch,O., Connolly,B.A., Steinhoff,H.J., McGregor,A., Goody,R.S. and Restle,T. (2000) HIV-1 reverse transcriptase-pseudoknot RNA aptamer interaction has a binding affinity in the low picomolar range coupled with high specificity. *J. Biol. Chem.*, **275**, 18271–18278.
73. Semizarov,D., Frost,L., Sarthy,A., Kroeger,P., Halbert,D.N. and Fesik,S.W. (2003) Specificity of short interfering RNA determined through gene expression signatures. *Proc. Natl Acad. Sci. USA*, **100**, 6347–6352.
74. Fedorov,Y., Anderson,E.M., Birmingham,A., Reynolds,A., Karpilow,J., Robinson,K., Leake,D., Marshall,W.S. and Khvorova,A. (2006) Off-target effects by siRNA can induce toxic phenotype. *RNA*, **12**, 1188–1196.
75. Innes,N.P. and Ogden,G.R. (1999) A technique for the study of endocytosis in human oral epithelial cells. *Arch. Oral Biol.*, **44**, 519–523.
76. Berezhna,S.Y., Supekova,L., Supek,F., Schultz,P.G. and Deniz,A.A. (2006) siRNA in human cells selectively localizes to target RNA sites. *Proc. Natl Acad. Sci. USA*, **103**, 7682–7687.
77. Gurney,T.,Jr and Eliceiri,G.L. (1980) Intracellular distribution of low molecular weight RNA species in HeLa cells. *J. Cell Biol.*, **87**, 398–403.
78. Wassarman,D.A. and Steitz,J.A. (1991) Structural analyses of the 7SK ribonucleoprotein (RNP), the most abundant human small RNP of unknown function. *Mol. Cell Biol.*, **11**, 3432–3445.
79. Matera,A.G. and Ward,D.C. (1993) Nucleoplasmic organization of small nuclear ribonucleoproteins in cultured human cells. *J. Cell Biol.*, **121**, 715–727.
80. Robb,G.B., Brown,K.M., Khurana,J. and Rana,T.M. (2005) Specific and potent RNAi in the nucleus of human cells. *Nature Struct. Mol. Biol.*, **12**, 133–137.
81. Haylett,T. and Thilo,L. (1991) Endosome-lysosome fusion at low temperature. *J. Biol. Chem.*, **266**, 8322–8327.
82. Dunn,W.A., Hubbard,A.L. and Aronson,N.N.,Jr (1980) Low temperature selectively inhibits fusion between pinocytic vesicles and lysosomes during heterophagy of 125I-asialofetuin by the perfused rat liver. *J. Biol. Chem.*, **255**, 5971–5978.
83. Drin,G., Cottin,S., Blanc,E., Rees,A.R. and Temsamani,J. (2003) Studies on the internalization mechanism of cationic cell-penetrating peptides. *J. Biol. Chem.*, **278**, 31192–31201.
84. Padari,K., Säälik,P., Hansen,M., Koppel,K., Raid,R., Langel,Ü. and Pooga,M. (2005) Cell transduction pathways of transportans. *Bioconjug. Chem.*, **16**, 1399–1410.
85. Sato,S.B., Taguchi,T., Yamashina,S. and Toyama,S. (1996) Wortmannin and Li^+ specifically inhibit clathrin-independent endocytic internalization of bulk fluid. *J. Biochem.*, **119**, 887–897.
86. Araki,N., Johnson,M.T. and Swanson,J.A. (1996) A role for phosphoinositide 3-kinase in the completion of macropinocytosis and phagocytosis by macrophages. *J. Cell Biol.*, **135**, 1249–1260.
87. Silverstein,S.C. (1977) Endocytic uptake of particles by mononuclear phagocytes and the penetration of obligate intracellular parasites. *Am. J. Trop. Med. Hyg.*, **26**, 161–169.
88. Stahlhut,M. and van Deurs,B. (2000) Identification of filamin as a novel ligand for caveolin-1: evidence for the organization of caveolin-1-associated membrane domains by the actin cytoskeleton. *Mol. Biol. Cell*, **11**, 325–337.
89. Brezis,M., Rosen,S., Silva,P., Spokes,K. and Epstein,F.H. (1984) Polyene toxicity in renal medulla: injury mediated by transport activity. *Science*, **224**, 66–68.
90. Zhang,A.Y., Yi,F., Zhang,G., Gulbins,E. and Li,P.L. (2006) Lipid raft clustering and redox signaling platform formation in coronary arterial endothelial cells. *Hypertension*, **47**, 74–80.
91. Simons,K. and Ikonen,E. (1997) Functional rafts in cell membranes. *Nature*, **387**, 569–572.
92. Gumbleton,M., Abulrob,A.G. and Campbell,L. (2000) Caveolae: an alternative membrane transport compartment. *Pharm. Res.*, **17**, 1035–1048.
93. Sieczkarski,S.B. and Whittaker,G.R. (2002) Dissecting virus entry via endocytosis. *J. Gen. Virol.*, **83**, 1535–1545.
94. Cohen,P., Holmes,C.F. and Tsukitani,Y. (1990) Okadaic acid: a new probe for the study of cellular regulation. *Trends Biochem. Sci.*, **15**, 98–102.
95. Parton,R.G., Joggerst,B. and Simons,K. (1994) Regulated internalization of caveolae. *J. Cell Biol.*, **127**, 1199–1215.
96. Thomsen,P., Roepstorff,K., Stahlhut,M. and van Deurs,B. (2002) Caveolae are highly immobile plasma membrane microdomains, which are not involved in constitutive endocytic trafficking. *Mol. Biol. Cell*, **13**, 238–250.
97. Maxfield,F.R. (1982) Weak bases and ionophores rapidly and reversibly raise the pH of endocytic vesicles in cultured mouse fibroblasts. *J. Cell Biol.*, **95**, 676–681.
98. Luthman,H. and Magnusson,G. (1983) High efficiency polyoma DNA transfection of chloroquine treated cells. *Nucleic Acids Res.*, **11**, 1295–1308.
99. Ciftci,K. and Levy,R.J. (2001) Enhanced plasmid DNA transfection with lysosomotropic agents in cultured fibroblasts. *Int. J. Pharm.*, **218**, 81–92.
100. Almofti,M.R., Harashima,H., Shinohara,Y., Almofti,A., Baba,Y. and Kiwada,H. (2003) Cationic liposome-mediated gene delivery: biophysical study and mechanism of internalization. *Arch. Biochem. Biophys.*, **410**, 246–253.
101. Prasad,T.K., Rangaraj,N. and Rao,N.M. (2005) Quantitative aspects of endocytic activity in lipid-mediated transfections. *FEBS Lett.*, **579**, 2635–2642.
102. Khalil,I.A., Kogure,K., Akita,H. and Harashima,H. (2006) Uptake pathways and subsequent intracellular trafficking in nonviral gene delivery. *Pharmacol. Rev.*, **58**, 32–45.
103. Säälik,P., Elmquist,A., Hansen,M., Padari,K., Saar,K., Viht,K., Langel,Ü. and Pooga,M. (2004) Protein cargo delivery properties of cell-penetrating peptides. A comparative study. *Bioconjug. Chem.*, **15**, 1246–1253.
104. Swanson,J.A. and Watts,C. (1995) Macropinocytosis. *Trends Cell Biol.*, **5**, 424–428.
105. Rejman,J., Oberle,V., Zuhorn,I.S. and Hoekstra,D. (2004) Size-dependent internalization of particles via the pathways of clathrin- and caveolae-mediated endocytosis. *Biochem. J.*, **377**, 159–169.